Effect of curvature and chirality for hydrogen storage in single-walled carbon nanotubes: A Combined *ab initio* and Monte Carlo investigation

Giannis Mpourmpakis and George E. Froudakis[a),b)]
Department of Chemistry, University of Crete, P.O. Box 1470, Heraklion, 71409 Crete, Greece

George P. Lithoxoos and Jannis Samios[a),c)]
Laboratory of Physical Chemistry, Department of Chemistry, University of Athens, Panepistimiopolis, 15771 Athens, Greece

(Received 9 November 2006; accepted 21 February 2007; published online 10 April 2007)

Combined *ab initio* and grand canonical Monte Carlo simulations have been performed to investigate the dependence of hydrogen storage in single-walled carbon nanotubes (SWCNTs) on both tube curvature and chirality. The *ab initio* calculations at the density functional level of theory can provide useful information about the nature of hydrogen adsorption in SWCNT selected sites and the binding under different curvatures and chiralities of the tube walls. Further to this, the grand canonical Monte Carlo atomistic simulation technique can model large-scale nanotube systems with different curvature and chiralities and reproduce their storage capacity by calculating the weight percentage of the adsorbed material (gravimetric density) under thermodynamic conditions of interest. The author's results have shown that with both computational techniques, the nanotube's curvature plays an important role in the storage process while the chirality of the tube plays none. © *2007 American Institute of Physics*. [DOI: 10.1063/1.2717170]

INTRODUCTION

It is well known that hydrogen is an ideal energy carrier and probably the fuel of the future. For several technological reasons, however, it has not been used in great extent up to now. In order to achieve a commercial and widespread use of hydrogen as a fuel and versatile energy carrier, feasible chemical technologies for storage systems[1–7] and large-scale hydrogen production[8–10] have to be developed.

In the beginning, metal alloys were tested for gas storage usage (e.g., H_2) but even though they have sufficient storage capacity, they are expensive and heavy for commercial production focused on mobile applications. On the other hand, high-pressure tanks are used now in automobiles, but the 400–700 bars pressure of hydrogen in the tanks makes their extensive use problematic for several technical reasons. In order to obtain high efficiency of the hydrogen storage, new materials such as activated carbons, carbon fibers, and monoliths, as well as single-walled nanotubes and nanohorns, etc., are continuously under investigation and test by several groups worldwide.

Concretely, after the discovery of carbon nanotubes,[11] numerous scientists focused their interest on this new material and a new branch of science was developed aimed at nanostructured materials with specific properties.[2–14] Note that the potential of carbon nanotubes as means for gas storage was understood from the beginning and a large number of experimental[1,15] and theoretical studies[16–21] have been devoted so far in order to explore their unique properties. In the past few years, especially the single-walled nanotubes (SWNTs) have been suggested as suitable materials for gas storage.

On the other hand, according to the U.S. Department of Energy (DOE),[22] the standardized targets for gravimetric density for gas storage and transportation is 6.5 wt %. So, research groups focused on the field started to test the storage capacity of tubular materials under different conditions, trying to reach the U.S. DOE target. We mention, however, that by comparing the results of all competing research groups we may easily figure out that they are controversial. One major reason is that a great variety of tubes are used and no relation has been established between the hydrogen adsorption and the tube characteristics (e.g., diameter type). To the best of our knowledge, Darkrim and Levesque were the first who computed hydrogen adsorption in SWNTs for various tube diameters and intertube spacing by using the well-known Monte Carlo (MC) technique.[16,23,24] The results obtained from those studies were promising enough to encourage many other researchers to study hydrogen adsorption further.[18–20,25–29] For more details, the reader is referred to recent very interesting reviews, summarizing experimental and theoretical studies on this particular topic.[4,20,21] As a result, the theoretical and experimental studies so far show that the problem of hydrogen adsorption in carbon nanotubes still remains quite challenging.

The main purpose of the present study is to model the adsorption of hydrogen in SWNTs with tubes of different diameters and types or, in other words, *curvature* and *chirality*, by using appropriate simulation techniques. With this treatment, we try to clarify theoretically the controversy of some results concerning the hydrogen adsorption capacity of similar systems obtained previously by other research

[a)]Author to whom correspondence should be addressed
[b)]Electronic mail: frudakis@chemistry.uoc.gr
[c)]Electronic mail: isamios@cc.uoa.gr

groups. It is obvious that theoretical calculations in this field can be extremely useful in attaining a thorough and quantitative understanding of the elementary steps concerning the gas adsorption/desorption phenomenon that takes place in the aforementioned materials.

Among the well-established computational techniques used to study hydrogen storage in porous materials are the density functional theory (DFT), which is a first principles quantum chemistry method and the grand canonical Monte Carlo (GCMC) simulation. Generally, the theoretical calculations employed in this research field can be classified according to the approximations that they are based on.[20] The different simulation methods adopted can be the second reason (the first is the different tube models used) for the controversial results in the theoretical studies. In the *ab initio* theoretical studies, both chemisorption[30,31] and physisorption[33–37] were investigated within the DFT method. Only with the use of high accuracy computational techniques we can understand the nature of the hydrogen interaction with the SWNts.[38]

By considering the computer simulation studies reported on the field so far, we mention that in order to study the hydrogen adsorption isotherms for such materials, the most appropriate method is the grand canonical Monte Carlo.[16,17] It should be also emphasized here that quantum effects depend on the mass and confinement of the adsorbed molecules inside the tubes, the temperature of storage and the density of the stored material. So, in order to account for the quantum effects of hydrogen in the process of storage, several research groups have employed the path integral GCMC simulation technique.[18,19,39] Furthermore, in some cases the molecular mechanics and molecular dynamics classical algorithms were also employed to explore specific problems to this interesting topic.

COMPUTATIONAL DETAILS

Ab initio

The aim of the *ab initio* study is to calculate the binding energy between the molecular hydrogen and the walls of carbon nanotubes of different diameters and chiralities. In order to treat our system with high accuracy *ab initio* methods without ending up in prohibitively large computations we applied the cluster approximation. For each SWNT, we produced an oriented and curved coronenelike graphene sheet model using a two phase process. At first, a polycyclic C_{24} cluster was obtained by means of cutting from the corresponding SWNT model. Secondly, the dangling bonds of the sp^2 hybridized C_{24} cluster were saturated by hydrogen atoms resulting in the $C_{24}H_{12}$ model cluster (Fig. 1).

A hydrogen molecule can approach the walls of a SWNT not only from outside (out), that is the most common case, but also from inside (in). On top of this there are three different binding sites: on top of a C atom (top), in the middle of a C–C bond (bridge), and in the center of a C hexagon (hollow). All these concern the tube walls morphology. In addition there are several approach orientations for the hydrogen molecule. We examined the most important of these which were for the bridge case; perpendicular (P), longitudinal (L), and transversal (T) configurations according to the C–C bond axis; two for the hollow case; perpendicular and longitudinal configurations according to the C–C axis of two antidiametric carbon atoms of the C hexagon; and one for the top case: the perpendicular configuration according to the SWNT's axis. If we consider for each site and configuration the inside and the outside cases, we end up in 12 different approaches of H_2 to the SWNT wall. For each case we investigate the SWNT-H_2 interaction by scanning the potential energy surface (PES).

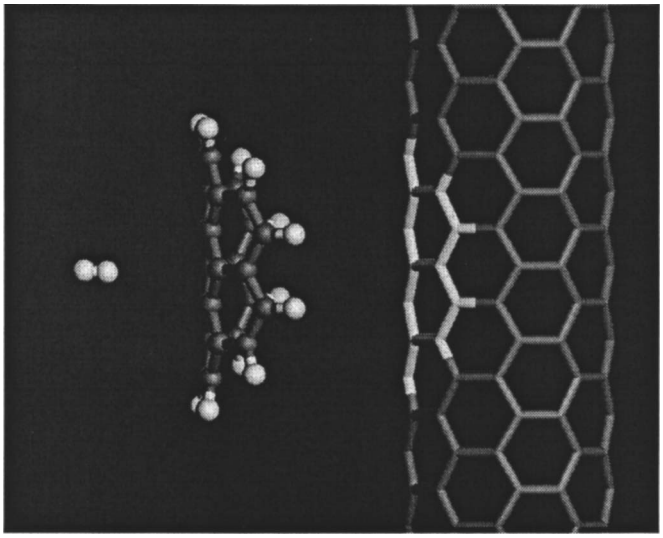

FIG. 1. $C_{24}H_{12}$ model cluster interacting with H_2 Hydrogen approaches the center of the hexagonal carbon ring with perpendicular to the tube's axis configuration.

The *ab initio* method used was the "Density functional theory" with the B3LYP (Ref. 39) hybrid functional and the calculations were performed using the GAUSSIAN 03 program package.[40] Targeting on high accuracy, we used two different basis sets in order to describe our system. The interacting hydrogen molecule together with the six neighboring carbon atoms were treated with larger basis set than the other atoms of the cluster. The large basis set was chosen to be of triple zeta quality plus polarization and diffusion functions for both heavy and light atoms (6-311++G^{**}) while the smaller one was the 3-21G. In a recent theoretical study[41] we demonstrated the performance of several functionals within the DFT, to calculate this very weak interaction, as well as the need of further correcting the obtained binding energy values by using the basis set superposition error (BSSE) correction. Despite the DFT is not in principle an appropriate method to describe the Van der Waals type of interactions, we showed that the obtained binding energy values using the B3LYP method and without applying the BSSE correction are very similar to the ones calculated at the CCSD level of approximation, including the BSSE corrections. Further to this, hydrogen coverage calculations in SWNTs using Langmuir isotherms based on the binding energy values calculated at the previously mentioned levels reproduced the existing experimental data. By this way, we managed to propose a functional which produces similar results with a very accurate level theory (CCSD) and is computationally very efficient to

TABLE I. SWNT types and corresponding geometries selected to study the adsorption phenomenon of molecular hydrogen by using the *NVT* MC and GCMC at different thermodynamic conditions.

Simulation Techniques	Type of SWNT	Diameter D (nm)	Height H (nm)
NVT MC and GCMC	(13,10)	1.564	5.67
NVT MC and GCMC	(11,11)	1.491	5.67
NVT MC and GCMC	(7,4)	0.755	5.67
NVT MC and GCMC	(6,6)	0.814	5.67

use. As already mentioned, the same functional (B3LYP) is use in the current study.

The physisorption energy of a H_2 molecule on the nanotube wall can be calculated as follows:

$$E_{\text{Physisorption}} = E_{C_{24}H_{12}-H_2} - E_{C_{24}H_{12}} - E_{H_2}, \quad (1)$$

where $E_{C_{24}H_{12}-H_2}$ is obtained from the scan of the potential energy of the SWNT-molecular hydrogen structure, $E_{C_{24}H_{12}}$ is the energy of the $C_{24}H_{12}$ cluster, and E_{H_2} is the energy of the H_2 molecule. For purposes of simplification we will refer $E_{\text{Physisorption}}$ as hydrogen's binding energy.

Grand canonical Monte Carlo

The simulation of the system at each thermodynamic point of interest has been performed according to the following two step procedure. In the beginning, we performed *NVT* Monte Carlo simulation in order to calculate the excess chemical potential using Widom's test particle method.[42] Further to this, we employed the GCMC simulation technique[17,43] following the Metropolis' sampling scheme. This method has been introduced in order to obtain, first of all the density profiles of the adsorbed hydrogen inside and outside of the tube surface and secondly, to estimate the adsorption capacity of the system in terms of the calculated weight percent (wt %) of hydrogen at the selected state points.

For the purpose of this work, we have selected to study the following types of SWNTs: (a) (13,10) chiral, (b) (11,11) armchair, (c) (7,4) chiral, and (d) (6,6) armchair. The geometric characteristics of the aforementioned type SWNTs are presented in Table I. From the geometric data of SWNTs given in this table, our intention to study the adsorption of hydrogen in carbon nanotubes with different chiralities and curvatures seems clear.

In each case, we have considered a model consisting of arrays of parallel nanotubes. The tubes studied are open-ended cylindrical structures, a characteristic that according to the literature lists them among the most promising adsorbent means for gases. So, hydrogen can be stored either internally or externally in the space between tubes. The amount of hydrogen that is stored is dependent on the attraction induced by the graphite carbon atoms on hydrogen molecules.

The simulation cell is made up of three rows of three tubes each, making up a total of nine parallel nanotubes. The tube spacing is $g=0.7$ nm. In each case, the lateral dimensions of the simulation cell are $L_x=L_y=3(g+D)$ and $L_z=H$.

TABLE II. Thermodynamic states of hydrogen studied by Monte Carlo simulations. (SC denotes supercritical state of matter.)

State points	T (K)	P (MPa)	Hydrogen density (Kg/m^3)	Thermodynamic state
A	175	0.1	0.138	SC
B	175	1.0	1.376	SC
C	175	5.0	6.679	SC
D	175	10.0	12.841	SC

A one site Lennard-Jones (LJ) potential, centered on the hydrogen molecule, describes the interactions between hydrogen molecules,

$$v_{LJ}(r) = 4\varepsilon\left[\left(\frac{\sigma}{r}\right)^{12} - \left(\frac{\sigma}{r}\right)^{6}\right], \quad (2)$$

with $\sigma=0.2958$ nm and $\varepsilon/k_B=36.7$ K (from Ref. 16)

For carbon-hydrogen interaction the LJ parameters are taken to be $\sigma=0.3179$ and $\varepsilon/k_B=32.17$ K (from Ref. 16).

The simulated thermodynamic state points (P,T,ρ) of hydrogen are summarized in Table II.

In each *NVT* MC simulation, corresponding to a different thermodynamic point, we created 10^6 steps in order to equilibrate the system and additionally 10^6 steps for the calculation of the chemical potential needed for the second level of the planned procedure of simulations. As far as the implementation of the GCMC simulations is concerned, we performed 10^6 MC steps for the system to reach equilibrium and after that approximately other 10^6 which have been spent to obtain statistical averages. The estimated statistical averages of the number of hydrogen molecules inserted and stabilized in the simulation cell for each thermodynamic state of interest are summarized in Table III.

RESULTS AND DISCUSSION

Ab initio

We calculated the binding energy by scanning the potential energy surface of hydrogen's approach to various carbon nanotube walls. The SWNTs were the (5,5), (6,6), (9,9), and (11,11) armchair-type nanotubes, which have different diameters and the (12,6) and (13,10) which have similar diameters with the corresponding (9,9) and (11,11) ones. We checked

TABLE III. Average numbers of hydrogen molecules $\langle N\rangle$ in the simulation cell inside and outside the tube surfaces for the four different types of SWNTs with defined diameters and heights, calculated at each thermodynamic state of interest by using the GCMC technique, from this study.

	Average number of hydrogen molecules $\langle N\rangle$			
State points	(13,10) SWNTs	(11,11) SWNTs	(7,4) SWNTs	(6,6) SWNTs
A	36	36	47	46
B	318	317	188	206
C	1102	1072	475	507
D	1648	1581	671	695

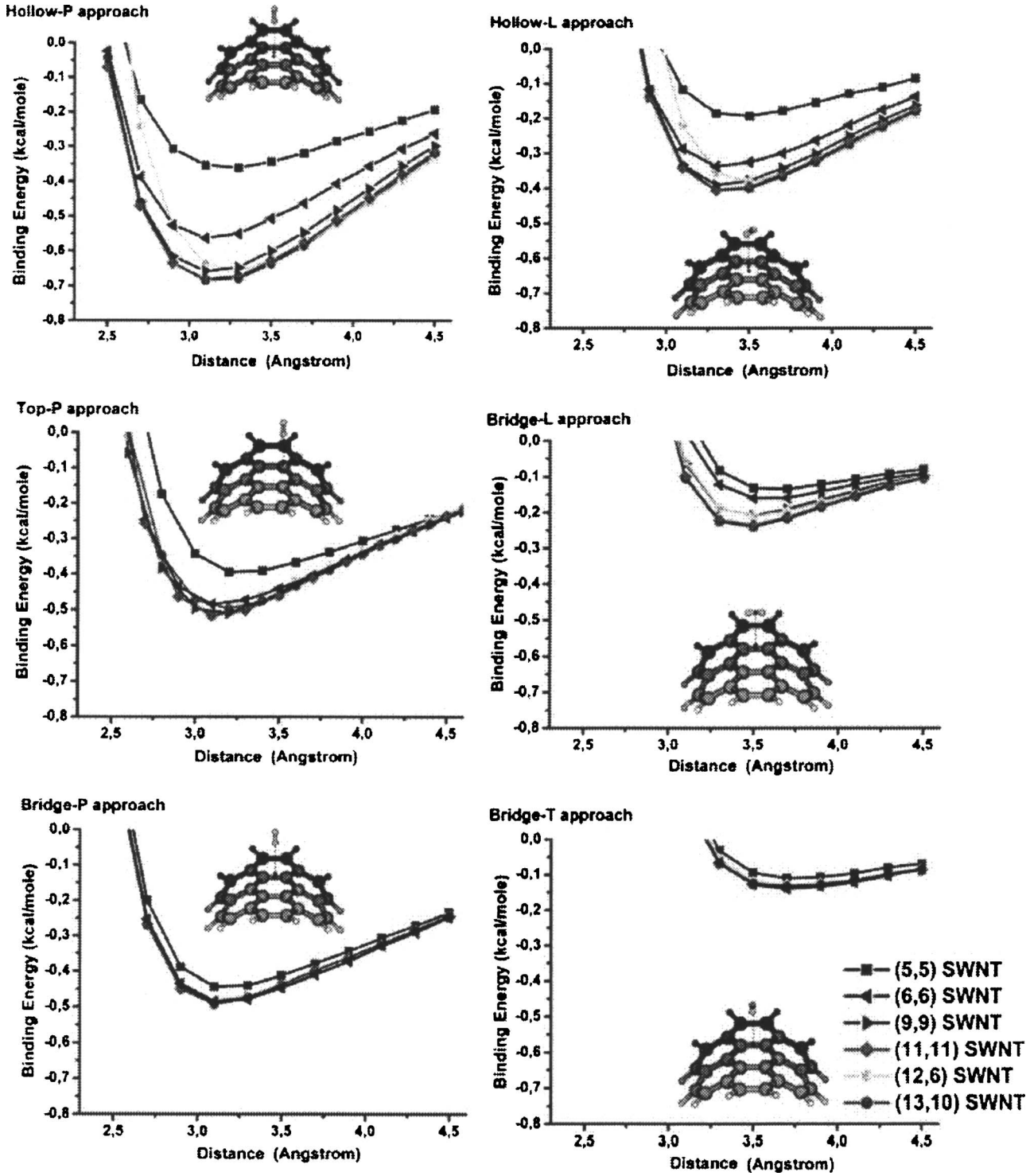

FIG. 2. Scan of the potential energy of hydrogen interacting with various SWNTs [(5,5), (6,6), (9,9), (11,11), (13,10), and (12,6)] with different approaches, concerning the sites of the tube walls (hollow, top, and bridge) and the configuration of H_2 (perpendicular, longitudinal, and transversal). The distance is defined from the tube walls.

six different approaches of hydrogen for all these SWNTs. These were the hollow approach (with hydrogen's perpendicular and longitudinal configuration), the top approach (with hydrogen's perpendicular configuration), and the bridge approach (with hydrogen's perpendicular, longitudinal, and transversal configuration). The results obtained from the PES scan are presented on Fig. 2.

A general observation for all the systems studied is that depending on the site of SWNT that hydrogen approaches and on the latter's configuration, hydrogen binds on tubes' walls with the following behavior:

$$\mathrm{BE}_{\text{hollow-P}} > \mathrm{BE}_{\text{top-P}} > \mathrm{BE}_{\text{bridge-P}} > \mathrm{BE}_{\text{hollow-L}} > \mathrm{BE}_{\text{bridge-L}} > \mathrm{BE}_{\text{bridge-T}}. \quad (3)$$

Note that only for the case of the (5,5) SWNT we found the

bridge-P configuration slightly more preferable than the hollow-P ($\Delta E=0,1$ Kcal/mol).

So, it is clear that hydrogen prefers to interact with the hollow position with perpendicular to the tube axis configuration. In this configuration hydrogen takes advantage of the π electrons of the hexagonal ring and forms small charged induced dipoles. This induced dipole had explained why H_2 prefers to interact with the outer walls of a (5,5) SWNT with perpendicular configurations regardless of the site of the approach.[34]

Some more interesting comments can be made on the physisorption of molecular hydrogen on the selected sites of the tube walls, the diameter, and chirality of the latter. We remind that the relation of the diameters of these nanotubes is the following:

$$D_{5,5} < D_{6-6} < D_{9-9} = D_{12-6} < D_{13-10} = D_{11-11}. \quad (4)$$

It is clear from Fig. 2 that attractive potential of hydrogen's binding starts at 2.5–2.7 Å while the most efficient binding is observed at 3.2 Å approximately, which is in agreement with other theoretical results.[32,35–37] The distance of this interaction does not depend on the type or the diameter of the SWNT and is the same for all the nanotubes. In addition, weaker interactions, such as the bridge-L and bridge-T curves, show their minimum in larger distances (3.5–3.7 Å) than the stronger hollow-P and top-P, which show their minimum in relative shorter distances (3.1–3.2 Å). More interestingly the binding energy between the molecular hydrogen and the carbon nanotubes depends on the curvature of the nanotubes and not on their chirality. As the curvature of the nanotube decreases the binding energy of the H_2 molecule increases, due to the fact that C atoms come closer to the molecular hydrogen contributing to a more efficient binding. Nanotubes of the same diameters and different chiralities binds the H_2 with the same energy [(9,9) compared with (12,6), and (11,11) compared with (13,10) SWNT]. The latter behavior was observed on all different approaches studied. Arellano *et al.*[36] calculated the hollow-P hydrogen's interaction with a (5,5) and (6,6) SWNTs' walls at −1.568 and −1.614 Kcal/mole respectively. We calculated this interaction at −0.361 and −0.563 kcal/mole which can be attributed to the fact that we did not include the whole nanotube system and that the local density approximation function they used does not describe the dispersion forces between molecules accurately, leading to overestimated binding energies.[32] Consequently our results are in agreement with the results of Arellano *et al.* showing that by increasing the nanotube diameter (5,5) $\rightarrow$(6,6), the hydrogen's binding energy increases.

Grand canonical Monte Carlo

As mentioned above, the main purpose of the present work has been the estimation of the adsorption capacity of molecular hydrogen in SWNTs, which are characterized by different curvatures and chiralities. We also mention that the height of all tubes studied was fixed at 5.67 nm, a height that is large enough in comparison to previous papers.[16] In addition the (13,10) chiral tube and the (11,11) armchair one have almost the same diameter ($D\cong 1.5$ nm) while the same gilts for the (7,4) chiral ($D=0.75$ nm) and for the (6,6) armchair tube ($D=0.81$ nm).

TABLE IV. The weight percentage of hydrogen molecules adsorbed outside and inside the tubes' surfaces for the four different types of SWNTs with defined diameters and heights, calculated at each thermodynamic state A, B, C, D by using the GCMC simulation technique from this work.

	Weight percentage of hydrogen molecules adsorbed in SWNTs (wt%)			
State points	(13,10) SWNTs	(11,11) SWNTs	(7,4) SWNTs	(6,6) SWNTs
A	0.06	0.06	0.17	0.15
B	0.55	0.57	0.67	0.68
C	1.92	1.92	1.70	1.67
D	2.87	2.83	2.40	2.29

According to our simulation results, molecular hydrogen can be adsorbed either internally or externally in the space between neighboring tubes as it can be clearly shown in various snapshots (see Fig. 6) of the simulation cell selected randomly after the equilibration of each system. From the GCMC simulation technique phase space production, we have calculated the weight percentage (wt %) of the adsorbed hydrogen as well as the density profile of hydrogen in the system for each simulated state point of interest.

The results concerning the weight percentage of the adsorbed supercritical fluid H_2 in SWNTs obtained from our simulations are summarized in Table IV.

By inspecting the results from this Table, we can clearly see that the (13,10) and (11,11) SWNTs, with same diameters, provide almost the same adsorption capacity for the state points A, B, C, and D which are characterized by a temperature of 175 K and pressures 0.1, 1.0, 5.0, and 10 Mpa, respectively. Concerning the adsorption capacity of (7,4) chiral and (6,6) armchair SWNTs, we can easily see that both systems provide the same wt % at each state, namely, A, B, C, and D.

In order to have a detailed picture at molecular level of how the adsorbed hydrogen is distributed inside and outside the nanotubes of different types, we have calculated the density profiles of adsorbed hydrogen for each system under investigation. The density profile was calculated according to concentric cylindrical shells histogram method, starting from the center of the simulation box, which coincides with the geometrical center of the central tube.

The density profiles for the (13,10) chiral and (11,11) armchair SWNTs at 175 K and various pressures in the range of 10–0.1 MPa obtained are presented in Fig. 3. By inspecting the corresponding diagrams from this figure, we can easily observe that a large amount of the adsorbed hydrogen is found inside the tube near the wall surface while H_2 close around the symmetry axe of the tube is significantly of smaller amount. In addition, a comparable amount of H_2

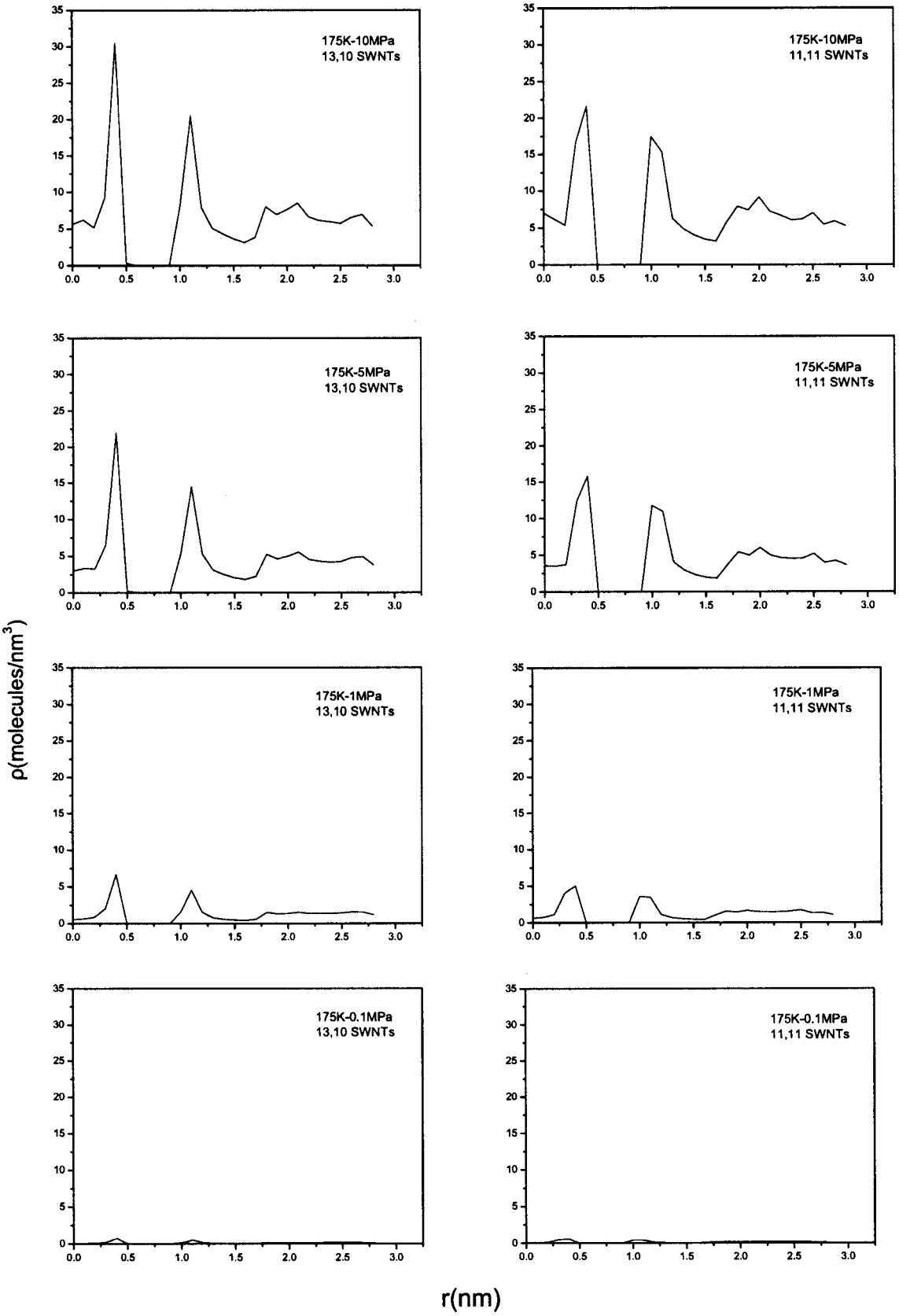

FIG. 3. Cylindrical density profiles of the adsorbed H_2 in (13,10) chiral and (11,11) armchair SWNTs at 175 K and pressure in the range of 10–0.1 MPa.

lies in the space between neighboring tubes.

For both the (6,6) and (7,4) SWNTs depicted in Fig. 4, we observe a relatively high number density close to the axis of the tube in comparison to that of the (13,10) and (11,11) ones. This is mainly due to the intermolecular interactions between hydrogen and the carbon atoms of the tube walls and the restricted inner tube space available for adsorption of the particles.

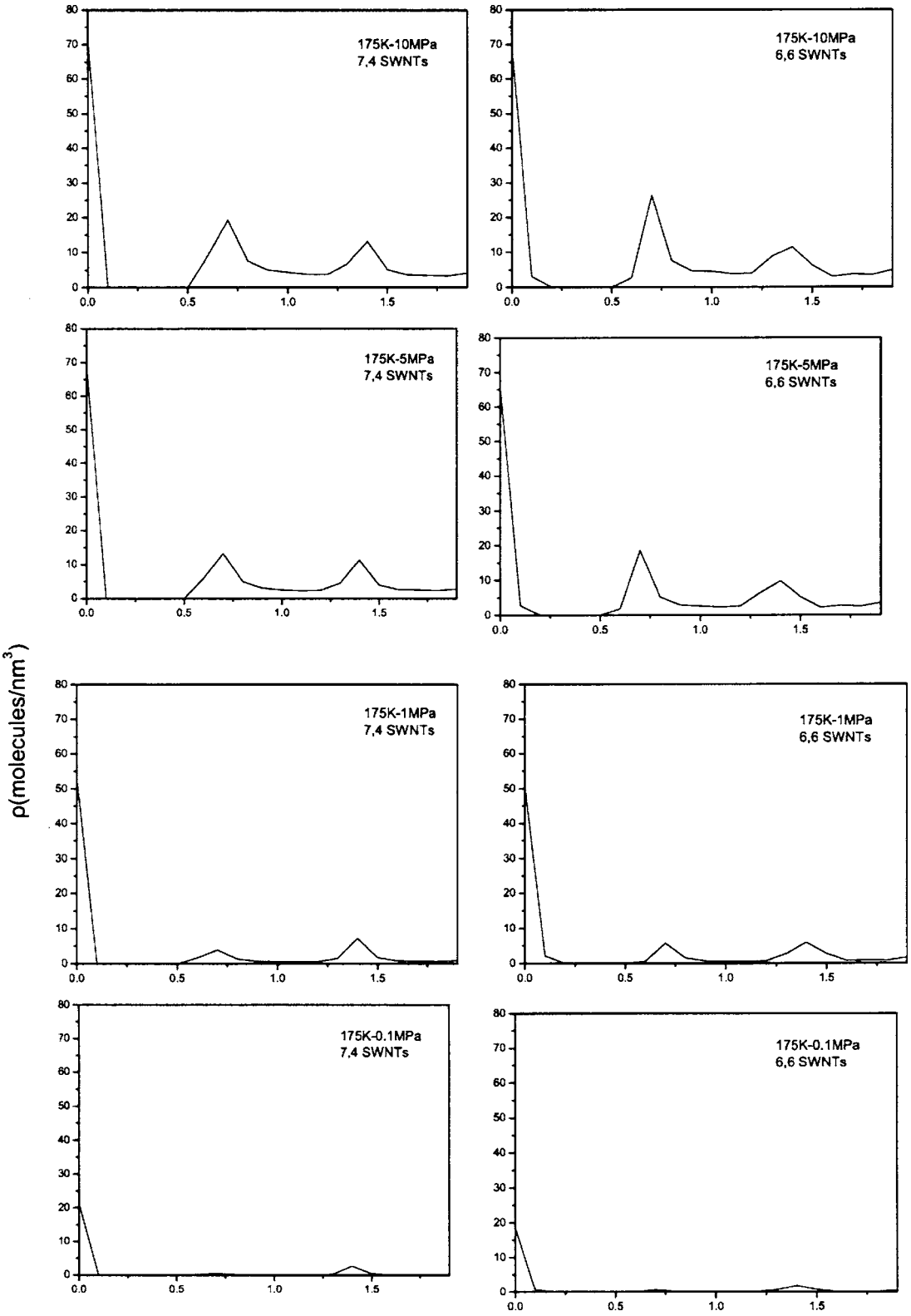

FIG. 4. Cylindrical density profiles of the adsorbed H_2 in (7,4) chiral and (6,6) armchair SWNTs at 175 K and pressure in the range of 10–0.1 MPa.

Finally, we also see from the density profiles that hydrogen presents similar distribution inside and outside the tubes for both chiral and armchair types of the same diameter.

To analyze further our adsorption results, we decided to employ appropriate theoretical considerations in order to describe, if possible, the adsorption isotherms obtained for the above-mentioned types of SWNTs in this study. As it was mentioned previously, the adsorption phenomenon investigated in the present study is based on interactions between the carbon atoms of the nanotubes and molecular hydrogen. The interactions involved are of the Van der Waals type and thus we are dealing with physisorption that is our main interest here.

It is well known from the literature, that there are vari-

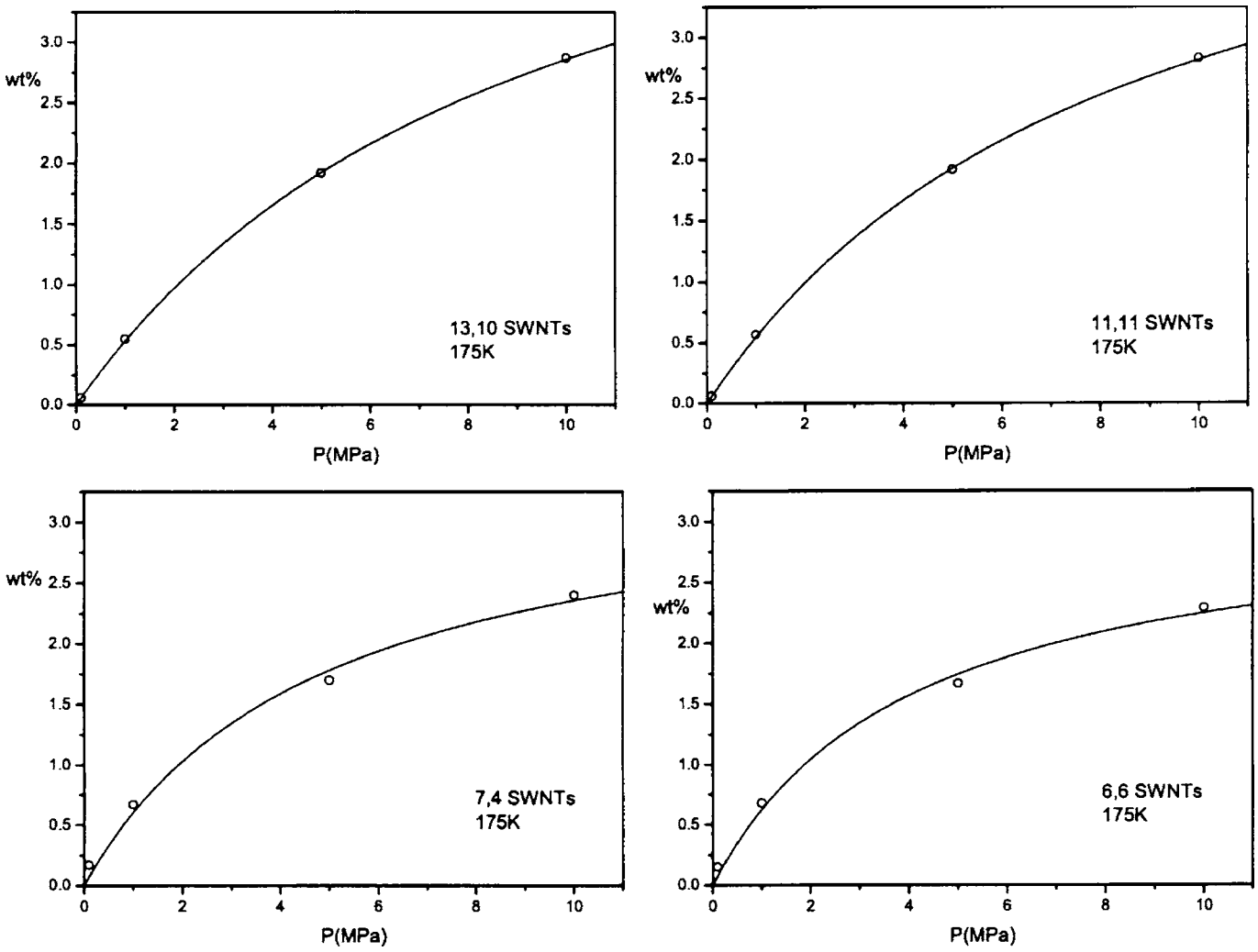

FIG. 5. Langmuir adsorption isotherms of H_2 vs pressure at 175 K for the (13,10) and (7,4) chiral as well as for the (11,11) and (6,6) armchair SWNTs from this work.

ous isotherms describing the physisorption phenomenon which have been categorized in six types (I–VI) proposed by Brunauer *et al.*[44] In the present study we found out that the adsorption isotherms obtained are well described by the well-known Langmuir theory, which is declared by the following equation:

$$\frac{\rho}{\rho_m} = \frac{B(T)P}{1 + B(T)P}, \tag{5}$$

where in our case ρ is the wt % of the adsorbed hydrogen in the adsorption material, ρ_m is the adsorption capacity corresponding to the saturation of the monolayer shell, P is the pressure of the system, and $B(T)$ is an empirical parameter which is depended on the temperature. An alternative form of the Langmuir isotherm can be expressed in the following relation:

$$\frac{P}{\rho} = \frac{1}{B(T)\rho_m} + \frac{P}{\rho_m}, \tag{6}$$

from which we can easily obtain ρ_m and $B(T)$.

By fitting the simulation results of Table IV to the above function, we obtained Langmuir isotherms at 175 K for both types of SWNTs, which are presented in Fig. 5. The theoretical saturation adsorption capacity values ρ_m obtained from the fit in the case of large diameter (13,10) and (11,11) SWNTs are 5.5% and 5.2%, respectively. In the case of (7,4) SWNTs we found ρ_m to be equal with 3.4%, while for the (6,6) one the estimated value is 3.1%. We mention at this point that our estimated ρ_m wt % values at 175 K for the (13,10) and (11,11) SWNTs with a diameter about 1.5 nm are comparable to the corresponding results reported in a previous simulation study of SWNTs at 150 K with a diameter 1.3 nm and tube spacing g equal to 0.6 nm.[17]

In order to obtain a visual perspective of the physisorption phenomenon of H_2 molecules in the aforementioned chiral and armchair SWNTs, we have selected some snapshots of representative configurations emphasizing the amount and the distribution profile of the adsorbed particles inside and outside the SWNT surfaces. Figure 6 shows eight snapshots of the adsorbed fluid in (13,10) and (7,4) chiral as well as in (11,11) and (6,6) armchair SWNTs at the isotherm of 175 K and for 1 and 10 MPa pressure. By inspecting these selected configurations we can easily confirm the behavior of the density profiles and Langmuir isotherms obtained from the employed procedure.

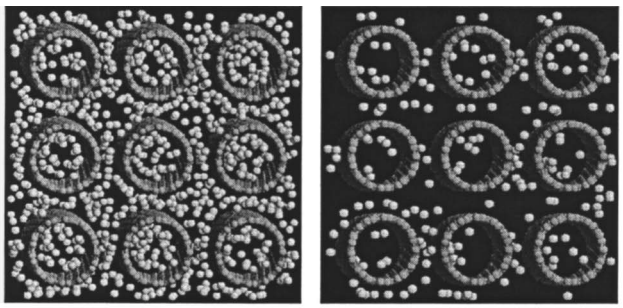

Snapshots of the simulation boxes for (13,10) SWNTs for P=10MPa (left) and P=1MPa (right)

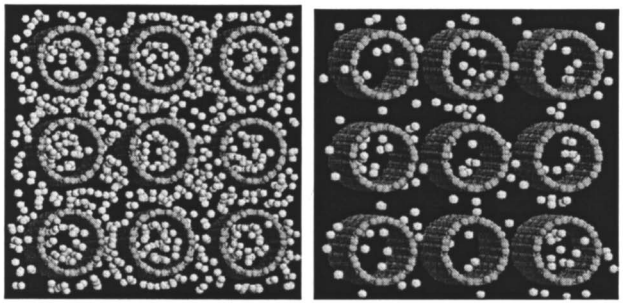

Snapshots of the simulation boxes for (11,11) SWNTs for P=10MPa (left) and P=1MPa (right)

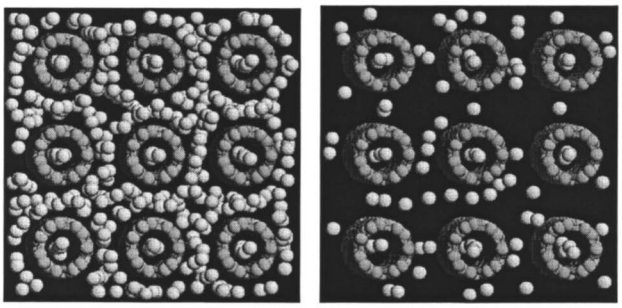

Snapshots of the simulation boxes for (7,4) SWNTs for P=10MPa (left) and P=1MPa (right)

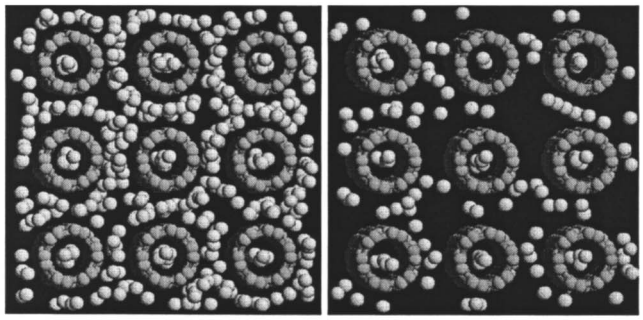

Snapshots of the simulation boxes for (6,6) SWNTs for P=10MPa (left) and P=1MPa (right)

FIG. 6. Snapshots of representative configurations from this GCMC simulations of H_2 adsorbed in SWNTs of different curvatures and chiralities.

CONCLUDING REMARKS

In this study, the *ab initio* method at the density functional level of theory (DFT) combined with the grand canonical Monte Carlo (GCMC) simulation technique have been employed to investigate the dependence of hydrogen storage in single-walled carbon nanotubes (SWCNTs) on both tube curvature and chirality. The use of *ab initio* DFT calculations provides in general useful information concerning the nature of hydrogen adsorption in SWCNTs selected sites and the binding under different curvatures and chiralities of the tube walls. On the other hand, the employment of the GCMC atomistic simulation technique can investigate the storage capacity in terms of the weight percentage (wt %) of the adsorbed material in large-scale nanotube systems as a function of curvature and chirality and of course at different thermodynamic conditions (P,T).

The results obtained from both computational techniques have shown that the nanotube's curvature plays an important role in the storage process while the chirality of the tube plays none.

ACKNOWLEDGMENTS

This study is supported through grants from the European Social Fund and National Resources. The authors

would like to thank the Ministry of Development (General Secretariat-GSRT) of the Greek government, for financial support of this research (IIENAΔ 03EΔ 181 and 548). Partial funding by the European Commission DG RTD (FP6 Integrated Project NESSHY, Contract No. SES6-518271) is gratefully acknowledged by the authors.

[1] A. C. Dillon, K. M. Jones, T. A. Bekkedakt, C. H. Kiang, D. S. Bethune, and M. J. Heben, Nature (London) **386**, 377 (1997).
[2] R. G. Ding, G. Q. Lu, Z. F. Yan, and M. A. Wilson, J. Nanosci. Nanotechnol. **1**, 7 (2001).
[3] A. C. Dillon and M. J. Heben, Appl. Phys. A: Mater. Sci. Process. **A72**, 133 (2001).
[4] F. L. Darkrim, P. Malbrunot, and G. P. Tartaglia, Int. J. Hydrogen Energy **27**, 193 (2002).
[5] A. D. Lan and A. Mukasyan, J. Phys. Chem. B **109**, 16011 (2005).
[6] B. Panella, M. Hirscher, and S. Roth, Carbon **43**, 2209 (2005).
[7] C. Liu and H. M. Cheng, J. Phys. D **38**, R231 (2005).
[8] *Hydrogen Energy System-Production and Utilization of Hydrogen and Future Aspects*, NATO ASI, Series E: Applied Sciences Vol. 295, edited by Y. Yuriim (Akcay, Turkey, 1994).
[9] E. Lyris, D. Argyropoulos, C. A. Mitsopoulou, D. Katakis, and E. Vrachnou, J. Photochem. Photobiol., A **108**, 51 (1997); S. Alvarez, R. Vicente, and R. Hoffmann, J. Am. Chem. Soc. **107**, 6253 (1985).
[10] J. Samios, D. Katakis, D. Dellis, E. Lyris, and C. A. Mitsopoulou, J. Chem. Soc., Faraday Trans. **94**, 3175 (1998).
[11] S. Iijima, Nature (London) **354**, 56 (1991).
[12] M. Terrones, W. K. Hsu, H. W. Kroto, and D. R. M. Walton, Top. Curr. Chem. **199**, 189 (1999).
[13] E. T. Thostenson, Z. Ren, and T.-W. Chou, Compos. Sci. Technol. **61**, 1899 (2001).
[14] M. Baxendale, J. Mater. Sci.: Mater. Electron. **14**, 657 (2003).
[15] A. C. Dillon, T. A. Bekkedahl, K. M. Jones, and M. J. Heben, Fullerenes **3**, 716 (1999).
[16] F. Darkrim and D. Levesque, J. Chem. Phys. **109**, 4981 (1998).
[17] D. Levesque, A. Gicquel, F. Darkrim, and S. Beyaz Kayiran, J. Phys.: Condens. Matter **14**, 9285 (2002); and G. Mpourmpakis, G. E. Froudakis, J. Samios, and G. P. Lithoxoos, Nano Lett. **6**, 1581 (2006).
[18] Q. Wang and J. K. Johnson, J. Phys. Chem. B **103**, 4809 (1999).
[19] Q. Wang and J. K. Johnson, J. Chem. Phys. **110**, 577 (1998).
[20] V. Meregalli and M. Parrinello, Appl. Phys. A: Mater. Sci. Process. **72**, 143 (2001); M. Becher, M. Haluska, M. Hirscher *et al.*, C. R. Phys. **4**, 1055 (2003).
[21] G. E. Froudakis, J. Phys.: Condens. Matter **14**, R453 (2002).
[22] S. Hynek, W. Fuller, and J. Bentley, Int. J. Hydrogen Energy **22**, 601 (1997).
[23] F. Darkrim and D. Levesque, J. Phys. Chem. B **104**, 6773 (2000).
[24] S. B. Kayiran, F. D. Lamari, and D. Levesque, J. Phys. Chem. B **108**, 15211 (2004).
[25] K. A. Williams and P. C. Ecklund, Chem. Phys. Lett. **320**, 352 (2000).
[26] H. Dodziuk and G. Dolgonos, Chem. Phys. Lett. **356**, 79 (2002).
[27] V. V. Simonyan, P. Diep, and J. K. Johnson, J. Chem. Phys. **111**, 9778 (1999).
[28] V. V. Simonyan and J. K. Johnson, J. Alloys Compd. **330**, 659 (2002).
[29] M. R. Smith, E. W. Bittner, W. Shi, J. K. Johnson, and B. C. Bockrath, J. Phys. Chem. B **107**, 3752 (2003).
[30] G. E. Froudakis, Nano Lett. **1**, 179 (2001).
[31] C. W. Bauschlicher, Jr., Nano Lett. **1**, 223 (2001); C. W. Bauschlicher, Jr. and C. R. So, *ibid.* **2**, 337 (2002).
[32] S. S. Han and H. M. Lee, Carbon **42**, 2169 (2004).
[33] X. R. Zhang, D. Cao, and J. Chen, J. Phys. Chem. B **107**, 4942 (2003).
[34] G. Mpourmpakis, E. Tylianakis, and G. Froudakis, J. Nanosci. Nanotechnol. **6**, 87 (2006).
[35] J. S. Arellano, L. M. Molina, A. Rubio, and J. A. Alonso, J. Chem. Phys. **112**, 8114 (2000).
[36] J. S. Arellano, L. M. Molina, A. Rubio, M. J. López, and J. A. Alonso, J. Chem. Phys. **117**, 2281 (2002).
[37] Y. Okamoto and Y. Miyamoto, J. Phys. Chem. B **105**, 3470 (2001); A. Ferre-Vilaplana, J. Chem. Phys. **122**, 214724 (2005).
[38] P. Kowalcchi, H. Tanaka, R. Holyst, K. Kaneto, T. Ohmori, and J. Miyamoto, J. Phys. Chem. B **109**, 17174 (2005).
[39] A. D. Becke, J. Chem. Phys. **98**, 5648 (1993); C. Lee, W. Yang, andR. G. Parr, Phys. Rev. B **37**, 785 (1988).
[40] M. J. Frisch *et al.*, GAUSSIAN 03, Revision B.02 (2003).
[41] G. Mpourmpakis and G. E. Froudakis (unpublished).
[42] G. L. Deitrick, L. E. Scriven, and H. T. Davis, J. Chem. Phys. **90**, 2370 (1989).
[43] *The Monte Carlo Methods in Condensed Matter Physics*, Topics in Applied Physics Vol. 71, edited by K. Binder (Springer, Berlin, 1995).
[44] S. Brunauer, L. S. Deming, W. S. Deming, and E. Teller, J. Am. Chem. Soc. **62**, 1723 (1940).